

MR hydrophysiology reveals multiple exchange pathways in neural tissue

Nathan Hu Williamson^{1,2}, Rea Ravin^{2,3}, Teddy Xuke Cai², Julian Alejandro Rey^{2,4}, and Peter Joel Basser²

¹Military Traumatic Brain Injury Initiative, Henry M Jackson Foundation for the Advancement of Military Medicine, Bethesda, MD, United States, ²Eunice Kennedy Shriver National Institute of Child Health and Human Development, Bethesda, MD, United States, ³Celoptics, Rockville, MD, United States, ⁴National Institute for General Medical Sciences, Bethesda, MD, United States

Synopsis

Keywords: Microstructure, Diffusion Modeling, Advanced diffusion encoding

Motivation: Understand the sensitivity of diffusion MRI to microstructure and function of living neural tissue.

Goal(s): Determine dominant exchange pathways and whether they are active or passive.

Approach: Realtime MR hydrophysiology was used to study steady-state water exchange and diffusion in live *ex vivo* neural tissue.

Results: Water exchange is not active *per se* but is linked to tonicity maintained by active transport. Tonicity modulates the apparent exchange rate between fast transmembrane and slow intracellular pathways. The transmembrane pathway has a high activation energy and does not require ions, suggesting it is not through channels or cotransporters but is likely through lipid bilayers.

Impact: A multisite exchange mechanism involving passive transmembrane and geometric pathways can explain connections to activity. Most of the transmembrane water exchange occurs through lipid bilayers in gray matter. This knowledge should inform the development of novel quantitative MRI biomarkers.

Introduction

Recent MR studies found significant water exchange in gray matter on 1–100 ms timescales.^{1–3} Some studies report that water actively cycles with ions through the Na⁺/K⁺-ATPase and downstream transporters, suggesting that water exchange is a potential biomarker for cellular metabolism and activity.^{4,6} But validation is challenging because no other method can provide the ground truth. We addressed this issue by developing MR hydrophysiology to understand the role of steady-state water exchange in water homeostasis *in vivo*.^{1,6–11} Here we perform drug, osmotic, ionic, and temperature perturbations to test the importance of various pathways for water exchange.

Methods

Ex vivo spinal cord samples were dissected from P1–P4 neonatal mice. Measurements were performed at 13.79 MHz with a low-field single-sided magnet (NMR MOUSE, Magritek)¹² and custom-built solenoid RF coil.¹ Diffusion was encoded in the *y*-direction (perpendicular to the cord) on sub-micron lengthscales (defined by the dephasing length $l_g = (D_0/g)^{1/3} \approx 800$ nm) and sub-millisecond timescales with spin echoes under a large static gradient (SG) $g = 15.3$ T/m.¹ Apparent diffusion coefficients in the *y*-direction were measured with 3 *b*-values varied from 0.096 to 1.5 ms/ μm^2 and are presented as percent change from baseline (ΔADC_y). Apparent exchange rates (*k*) were measured with two diffusion encodings separated by a mixing time following the diffusion exchange ratio (DEXR) method with $b_1 + b_2 = 4.5$ ms/ μm^2 and t_m varied from 0.2 to 300 ms.^{8,11} The sample chamber provided oxygenated artificial cerebrospinal fluid (aCSF) circulation (necessary for maintaining sample viability) and temperature control (by heat exchange with water baths). A three-site exchange model following an operator formalism¹³ faithfully simulated DEXR data.

Results and Discussion

Inhibition of the primary active transporter, Na⁺/K⁺-ATPase, with the drug ouabain reduced *k* from 140 s⁻¹ to 40 s⁻¹ (Figure 1 B,D). Previous studies interpreted this strong effect of ouabain as evidence of active water cycling.^{4,6} However, Na⁺/K⁺-ATPase inhibition also causes hypotonicity shown by ΔADC_y decreasing (Figure 1 B,C). To compensate for tonicity, we used aCSF in which the major ionic component, 128 mM NaCl, was replaced with 257 mM sucrose. If water actively cycles along with ions, then this should decrease *k*. Instead, *k* increased (Figure 1 A,D). ΔADC_y also increased, suggesting hypertonicity (Figure 1 A,C). Adding ouabain on top of 0 NaCl, 257 mM sucrose aCSF had no additional effect. Flipping the order of perturbations yielded similar results (Figure 1 B,C,D). Therefore, *k* is not linked to ion transport or Na⁺/K⁺-ATPase activity *per se*, but rather to the tonicity which is established by its activity.

Tonicity was perturbed by adding osmolytes incrementally from 0–200 mM (Figure 2). On normal samples, sucrose increased ΔADC_y and *k* only slightly (Figure 2 A,C,E). For ouabain-treated samples, 100 mM increased ΔADC_y and *k* to near-normal values but then 200 mM had no additional effect (Figure 2 B,C,E). Similar effects from mannitol (a smaller osmolyte) confirm the link to tonicity (Figure 2 D,C,E).

While not possible with *k* alone, the correlation between ΔADC_y and Δk does distinguish normal and ouabain-treated sample data (Figure 2 F). Normal sample data clustered due to homeostatic compensation of osmolarity. Ouabain-treated sample data showed a sigmoidal relationship. The two correlations do not overlap.

Temperature perturbations were also explored and reveal distinct activation energies E_a (Figure 3), fit as:

$$k = A \exp(-E_a/RT) \quad (\text{Eq. 1})$$

where *A*, *R*, and *T* are the pre-exponential factor, ideal gas constant, and absolute temperature. E_a was similar between the normal samples and normal +100 mOsm samples, but higher than ouabain-treated samples (Figure 3 H). E_a recovered when +100 mOsm was added to ouabain-treated samples, confirming the link to tonicity. Data across conditions were described by

$$\ln(A) = m \times E_a + \ln(A') \quad (\text{Eq. 2})$$

and

$$k = A' \exp(-E_a/R(1/T - 1/T_c)) \quad (\text{Eq. 3})$$

with a common crossover temperature $T_c = 1/(m \times R)$ (Figure 4 A,B). Other heterogeneous systems have exhibited this “Entropy—enthalpy compensation” (EEC) behavior.¹⁴⁻¹⁶ EEC is consistent with multisite exchange pathways. Supporting this mechanism, the 3-site exchange model predicts similar behavior (Figure 4 C,D).

In the 3-site exchange model, tonicity affects the ECS volume fraction which in turn modulates the sensitivity of k to geometric and transmembrane exchange pathways (Figure 5). The geometric pathway has a lower E_a near values for water self-diffusion.¹⁷ This is consistent with exchange along branching processes or between soma and processes.¹⁸⁻²⁰ The transmembrane pathway has a higher E_a but does not require ions, meaning it is not through channels or cotransporters and is likely through lipid bilayers.

Conclusion

Findings suggest exchange is related indirectly to activity but directly to tonicity via a multisite exchange mechanism. This fills gaps in our understanding of what diffusion and exchange measurements are (and could be) sensitive to in heterogeneous tissues, specifically gray matter.

Acknowledgements

This research was supported by the *Eunice Kennedy Shriver* National Institute of Child Health and Human Development Intramural Research Program.

References

- Williamson NH, Ravin R, Benjamini D, Merkle H, Falgairolle M, O'Donovan MJ, et al. Magnetic resonance measurements of cellular and sub-cellular membrane structures in live and fixed neural tissue. *Elife*. 2019;8:e51101.
- Jelescu IO, de Skowronski A, Geffroy F, Palombo M, Novikov DS. Neurite Exchange Imaging (NEXI): A minimal model of diffusion in gray matter with inter-compartment water exchange. *NeuroImage*. 2022;256:119277.
- Olesen JL, Østergaard L, Shemesh N, Jespersen SN. Diffusion time dependence, power-law scaling, and exchange in gray matter. *NeuroImage*. 2022;251:118976.
- Bai R, Springer Jr CS, Plenz D, Basser PJ. Fast, Na⁺/K⁺ pump driven, steady-state transcytolemmal water exchange in neuronal tissue: A study of rat brain cortical cultures. *Magnetic resonance in medicine*. 2018;79(6):3207-17.
- Springer Jr CS. Using 1H2O MR to measure and map sodium pump activity in vivo. *Journal of Magnetic Resonance*. 2018;291:110-26.
- Williamson NH, Ravin R, Cai TX, Falgairolle M, O'Donovan MJ, Basser PJ. Water exchange rates measure active transport and homeostasis in neural tissue. *PNAS nexus*. 2023;2(3):pgad056.
- Cai TX, Benjamini D, Komlos ME, Basser PJ, Williamson NH. Rapid detection of the presence of diffusion exchange. *Journal of Magnetic Resonance*. 2018;297:17-22.
- Williamson NH, Ravin R, Cai TX, Benjamini D, Falgairolle M, O'Donovan MJ, Basser PJ. Real-time measurement of diffusion exchange rate in biological tissue. *Journal of Magnetic Resonance*. 2020;317:106782.
- Cai TX, Williamson NH, Ravin R, Basser PJ. Disentangling the effects of restriction and exchange with diffusion exchange spectroscopy. *Frontiers in physics*. 2022;10:805793.
- Williamson NH, Witherspoon VJ, Cai TX, Ravin R, Horkay F, Basser PJ. Low-field, high-gradient NMR shows diffusion contrast consistent with localization or motional averaging of water near surfaces. *Magnetic Resonance Letters*. 2023;3(2):90-107.
- Cai TX, Williamson NH, Ravin R, Basser PJ. The Diffusion Exchange Ratio (DEXR): A minimal sampling of diffusion exchange spectroscopy to probe exchange, restriction, and time-dependence. *Journal of Magnetic Resonance*. 2024;366:107745.
- Eidmann G, Savelsberg R, Blümli P, Blümich B. The NMR MOUSE, a mobile universal surface explorer. *Journal of Magnetic Resonance, Series A*. 1996;122(1):104-9.
- Dortch R, Horch R, Does M. Development, simulation, and validation of NMR relaxation-based exchange measurements. *The Journal of chemical physics*. 2009;131(16).
- Daoukaki-Diamanti D, Pissis P, Boudouris G. Depolarization thermocurrents in frozen aqueous solutions of mono-and di-saccharides. *Chemical physics*. 1984;91(2):315-25.
- Sun WQ. Dielectric relaxation of water and water-plasticized biomolecules in relation to cellular water organization, cytoplasmic viscosity, and desiccation tolerance in recalcitrant seed tissues. *Plant Physiology*. 2000;124(3):1203-16.
- Psurek T, Soles CL, Page KA, Cicerone MT, Douglas JF. Quantifying changes in the high-frequency dynamics of mixtures by dielectric spectroscopy. *The Journal of Physical Chemistry B*. 2008;112(50):15980-90.

17. Mills R. Self-diffusion in normal and heavy water in the range 1-45. deg. The Journal of Physical Chemistry. 1973;77(5):685-8.

18. Palombo M, Ianus A, Guerrerri M, Nunes D, Alexander DC, Shemesh N, Zhang H. SANDI: a compartment-based model for non-invasive apparent soma and neurite imaging by diffusion MRI. Neuroimage. 2020;215:116835.

19. Khateri M, Reisert M, Sierra A, Tohka J, Kiselev VG. What does FEXI measure? NMR in Biomedicine. 2022;35(12):e4804.

20. Ianus A, Alexander DC, Zhang H, Palombo M. Mapping complex cell morphology in the grey matter with double diffusion encoding MR: A simulation study. Neuroimage. 2021;241:118424.

Figures

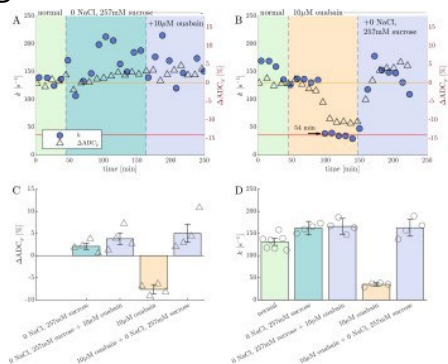


Figure 1. Exchange rate is not directly linked to active water cycling. A) Representative recording of k and percent change in apparent diffusion coefficient in the y -direction ΔADC_y during perturbations with aCSF in which NaCl was replaced with equimolar concentration of osmolyte (0 NaCl, 257 mM sucrose aCSF) and 10 μ M ouabain. B) Flipping the perturbation order by first adding 10 μ M ouabain and then washing to 0 NaCl, 257 mM sucrose aCSF with 10 μ M ouabain still present. c,d) Box plots of ΔADC_y and k under the various conditions. Each symbol represents a sample ($n=4$).

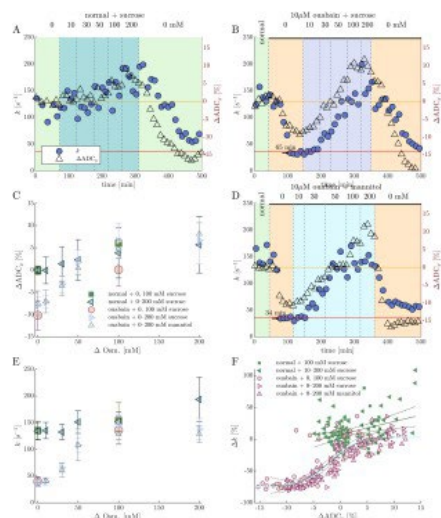


Figure 2. Exchange rate depends on tonicity. A,B,D) Recordings during osmotic perturbations with (A,B) sucrose or (D) mannitol on representative (A) normal or (B,D) ouabain-treated samples. C,E) Means (symbols) and SDs (error bars) across samples ($n=3$), including data from adding 100 mM sucrose in one step ($n=5$). F) Correlations between ΔADC_y and Δk . Predicted means and 99% CI (solid and broken lines) from regression of 1st (combined normal samples) and 5th (combined ouabain-treated samples) order polynomials. The latter is like a sigmoidal logistics function (aqua blue line).

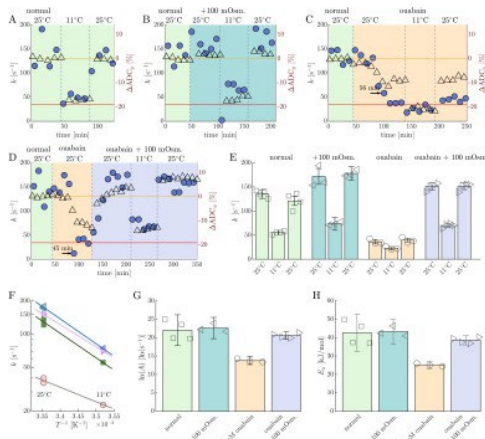


Figure 3. Tonicity affects activation energies of exchange. A-D) Representative recordings during temperature perturbation from 25°C to 11°C back to 25°C for each condition. E) Results of k from samples under normal ($n = 4$), + 100 mOsm ($n = 3$), 10 μ M ouabain ($n = 3$), and 10 μ M ouabain + 100 mOsm ($n = 4$) conditions. F) Arrhenius (semi-log) plot of the inverse of the absolute temperature T^{-1} vs. k averaged for each condition. Solid lines show averages of Arrhenius model fits (Eq. 1). G,H) Bar graphs of the natural log of pre-exponential factor A and activation energy E_a estimated from Eq. 1.

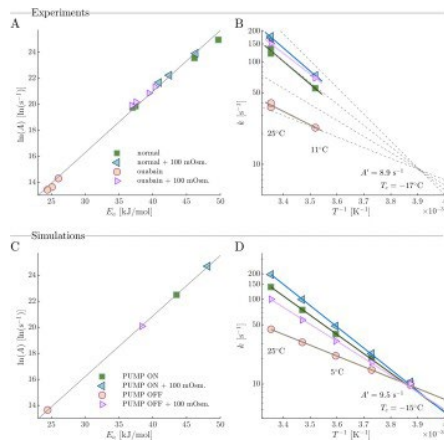


Figure 4. EEC behavior suggests a mechanism involving modulation of multisite exchange pathways by tonicity A) Experimental E_a vs. $\ln(A)$ for all samples showing a linear dependence described by Eq. 2 with $m = 0.470 \ln(s^{-1})/(kJ/mol)$ and $\ln(A) = 2.18 \ln(s^{-1})$. B) Semi-log plot of Eq. 3 for a range of E_a with $T_c = -17^\circ C$. Data from Fig. 4 F is also shown. C) E_a vs. $\ln(A)$ from 3-site model simulations with the Na^+/K^+ PUMP ON or OFF, without or with 100 mOsm. D) 3- site model predictions of k at temperatures between -25 and $+25^\circ C$ for the simulated conditions, along with predictions for Eq. 3 with $T_c = -15^\circ C$.

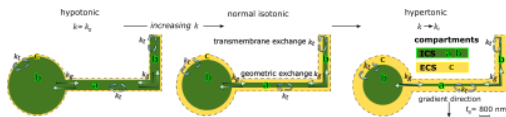


Figure 5. A 3-site exchange model for gray matter. Intracellular space (ICS) compartment a represents cellular processes oriented perpendicular to the gradient direction. ICS compartment b represents soma and processes oriented parallel to the gradient direction. Compartment c represents extracellular space (ECS). Compared to b and c, water in a is less mobile in the gradient direction due to diameters of processes being similar to the dephasing length, l_g . k_t is transmembrane exchange between ECS and ICS: a-c and b-c. k_g is geometric exchange between ICS compartments: a-b.